

Selenium-induced redox imbalance triggers oxidative DNA damage and the p53-dependent apoptosis of CHL-1 human melanoma cells

MAYSA ALHAWAMDEH¹, BUSHRA SARAIREH¹ and MOHAMED MOHSEEN WALY²

¹Department of Medical Laboratory Sciences, Faculty of Allied Medical Sciences, Mutah University, Al Karak 61710, Jordan; ²The Biotechnology and Genetic Engineering Program, Faculty of Science, Helwan National University, Helwan Sharkeya, Cairo Governate 4037120, Egypt

Received January 15, 2026; Accepted April 6, 2026

DOI: 10.3892/wasj.2026.469

Abstract. Melanoma, an aggressive type of cancer, is known for its ability to adapt to redox changes and resist standard treatments. Targeting the inherent redox weaknesses of melanoma has become a promising approach in research on redox-based cancer therapies. The present study investigated the toxic and DNA-damaging effects of elemental selenium (Se⁰) on CHL-1 human melanoma cells and its effects on p53-related cell death pathways. Cell survival was assessed using an MTT assay. Oxidative DNA damage was measured with the alkaline comet assay, which involved calculating the olive tail moment (OTM) and the percentage of tail DNA (% tail DNA). In addition, the expression levels of the genes *p53*, *p21*, *caspase-3* and *Bcl-2* were measured using reverse transcription-quantitative PCR. Hydrogen peroxide (H₂O₂) was used to induce oxidative stress, permitting the assessment of redox sensitization. Exposure to Se⁰ reduced CHL-1 cell viability, which is based on both the concentration and duration of exposure; the IC₅₀ value was determined to be 7.50 μM after 48 h. The results revealed that the combination of Se⁰ and hydrogen peroxide produced more oxidative DNA damage than either treatment alone, due to increasing levels of oxidative stress, as indicated by significant increases in OTM and % tail DNA. Selenium-induced oxidative DNA damage was associated with the activation of *p53*, *p21*, and *caspase-3*, and the significantly downregulation of *Bcl-2*, combined with the activation of p53-mediated cell cycle arrest and intrinsic pathways for apoptosis. The findings of the present study suggest that selenium may promote redox imbalance and oxidative damage in CHL-1 melanoma cells by activating the p53-regulated apoptotic signaling

pathway. Therefore, additional investigations are warranted in later-stage preclinical models to recognize the role of selenium as a redox-modulating agent that may increase the susceptibility of melanoma cells to oxidative stress.

Introduction

Melanoma, a highly aggressive and difficult-to-treat type of skin cancer, continues to be a major cause of skin cancer-related mortality worldwide. Recent Global Burden of Disease data suggest that the number of melanoma cases and deaths is expected to increase until 2044. This highlights differences among countries, underscoring the need for treatments that target specific mechanisms (1). The ability of the cancer to spread, its natural resistance to standard chemotherapy, and its frequent return following treatment are still major challenges in clinical practice. However, the use of targeted therapies, such as monoclonal antibodies and checkpoint inhibitors, has significantly improved short-term results for patients. A number of patients experience limited response times to therapy, which is sometimes due to either resistance or the toxic effects of these therapies. Thus, additional or alternative methods for selectively eliminating melanoma cells need to be developed based on established, well-characterized biological mechanisms (2,3).

Recent evidence suggests that redox dysregulation is a major factor in melanoma development. Compared to normal melanocytes, melanoma cells have significantly higher levels of reactive oxygen species (ROS). These advanced levels of ROS can result from any stimuli, including oncogenic signaling pathways, dysfunctional mitochondria, and metabolic changes in melanoma cells. Although the management of ROS levels in cancer cells favorably affects their development and survival, excessive oxidative stress can damage macromolecules (e.g., DNA, proteins, and lipids) and induce cell death signaling in melanoma cells. Emerging agents are being developed that treat this weakness by enhancing oxidative stress rather than the 'adaptive' capacity for melanoma cells (4,5).

DNA is highly vulnerable to oxidative damage caused by ROS. ROS induce oxidative damage, activating three signaling cascades that regulate the response of cells to oxidative

Correspondence to: Dr Maysa Alhawamdeh, Department of Medical Laboratory Sciences, Faculty of Allied Medical Sciences, Mutah University, Mutah Street, Al Karak 61710, Jordan
E-mail: maysa5005@mutah.edu.jo

Key words: melanoma, elemental selenium, oxidative stress, DNA damage, comet assay, p53 signaling, apoptosis

damage. This group of signaling pathways, the DNA damage response (DDR), primarily coordinates the cellular response to DNA damage (cell cycle arrest, DNA repair, or apoptosis) based on the type and severity of the DNA damage. The p53 tumor-suppressor protein is a major regulator of the cellular response to DNA damage and regulates the cellular response through downstream effector proteins (e.g., the p53-regulated genes that include p21 (*CDKN1A*) and caspases (e.g., *caspase-3*). Patients with melanoma exhibited the dysregulation of p53 signaling pathways and the levels of the p53-inhibitory protein, Bcl-2, which led to the unregulated growth and/or survival of melanoma cells and resistance to apoptosis. Substances that restore systems and regulate the functions of the body are a critical aspect of scientific study (6,7).

The present study aimed to determine whether the selenium-induced interruption of the balance of redox reactions, or redox imbalance, can lead to DNA damage caused by oxidative stress and the subsequent activation of p53-dependent apoptosis pathways in the melanoma cell line studied. In the present study, the redox-modulating ability of elemental selenium (Se^0) was assessed; Se^0 has different physical and chemical properties (e.g., solubility and cellular absorption rates) compared to other inorganic selenium species, such as sodium selenite. According to its physical and chemical properties, Se^0 has extremely limited solubility in water and very unique redox properties; therefore, Se^0 can provide insight into the mechanisms through which selenium alters the oxidative stress cellular process without being subject to the same interfering effects that occur with selenium salts (that is, with easily absorbed soluble inorganic selenium species). Selenium is necessary for synthesizing selenoproteins; selenoproteins play a crucial role in maintaining the oxidative process in the cells (i.e., balancing oxidative and antioxidant processes). Selenium compounds exhibit a concentration-dependent impact in biological systems at physiological concentrations. They serve as antioxidants at higher concentrations; selenium species can function as pro-oxidants, increasing the production of ROS. This functional transition, contingent upon concentration, is of particular significance in cancer research. The redox balance of cells can be altered by changes in the redox balance (8,9), determining whether a cell will survive or undergo apoptosis (8,9). The majority of experimental studies have been conducted on soluble inorganic selenium species, such as sodium selenite, due to their well-characterized redox activity and the generation of intracellular ROS (10-12). Multiple cancer models have identified the cytotoxicity and pro-apoptotic effects associated with selenium; however, other studies have focused on melanoma, and the only endpoints evaluated were single-cell viability and/or a single cellular marker (13,14). Few studies have comprehensively integrated quantitative oxidative DNA damage assessments with coordinated analyses of apoptosis-associated gene expression within the same experimental framework (15,16).

To the best of our knowledge, no study to date has systematically combined the functional evaluation of cytotoxicity, the quantitative comet-based assessment of genotoxicity, and coordinated p53 pathway-based gene expression profiles in the CHL-1 melanoma model. The present study presents mechanistic support for the association between Se^0 -induced redox imbalance, the production of oxidative DNA damage,

and the transduction of p53-dependent apoptotic signaling by integrating these three complementary endpoints within a single experimental framework (17,18).

The antioxidant defenses created by certain melanoma cells have the capacity to survive for an extended period of time following treatment, longer than would otherwise be expected due to their enhanced ability to buffer against oxidative damage and redox damage. Hydrogen peroxide (H_2O_2) is the most common experimental inducer of oxidative stress *in vitro*. Therefore, the purpose of using H_2O_2 along with Se^0 in the present study was to evaluate whether Se^0 can diminish the redox resistance of melanoma cells, thereby increasing susceptibility to oxidative DNA damage and genotoxic stress (19). Consequently, the incorporation of exogenous H_2O_2 constitutes a crucial experimental element, designed to replicate the oxidative stress characteristic of the tumor microenvironment. This methodology investigates selenium under conventional laboratory conditions and assesses the capacity of selenium to diminish the oxidative tolerance exhibited by melanoma cells. Consequently, this enhances their susceptibility to subsequent oxidative insult. This particular design choice reinforces the mechanistic understanding of selenium as a potential redox-sensitizing agent.

The CHL-1 human melanoma cell line was selected. It has been used in studies investigating how melanoma cells respond to oxidative stress and DNA damage (20,21), and its redox-adapted characteristics are well-known. Its ability to adapt to redox changes and its aggressive nature render it a good model for studying the mechanisms through which selenium affects redox processes (7). Therefore, the present study examined how Se^0 affects CHL-1 melanoma cells under normal and oxidative stress conditions. Cell viability was measured using the 3-(4,5-dimethylthiazol-2-yl)-2,5-diphenyl tetrazolium bromide (MTT) assay to determine how cytotoxicity changes with time and dose and to calculate the half-maximal inhibitory concentration (IC_{50}). Using the alkaline comet assay to quantify oxidative DNA damage via the olive tail moment (OTM) and the percentage of tail DNA (% Tail DNA), as well as using concurrent quantitative gene expression analysis for key regulators of DNA damage response and apoptosis (*p53*, *p21*, *caspase-3*, and *Bcl-2*), this dual approach allows for the systematic mechanistic assessment of redox modifications associated with exposure to Se^0 and apoptosis-related signaling pathways in melanoma cells.

Materials and methods

Preparation of selenium. Selenium powder (Se^0 ; CAS no. 7782-49-2; $\geq 99\%$ purity; cat. no. 229865; MilliporeSigma) was freshly prepared as a nominal stock suspension prior to each experiment. As Se^0 exhibits very limited aqueous solubility, it was prepared as a uniformly dispersed suspension rather than a true solution.

A suspension stock was prepared at a nominal concentration of 10 mM. Accurately measured, 7.9 mg of selenium powder was located in an amber sterile tube. The selenium powder was diluted in 500 μl absolute ethanol (100%) and mixed in a vortex mixer for 1 min to form a solution. The suspension was sonicated in a water bath sonicator for 10-15 min at room temperature (25°C) to promote uniform particle size

and reduce particle agglomeration. Following sonication, an appropriate volume of 9.5 ml of sterile complete culture medium (DMEM supplemented with 10% FBS, 100 U/ml penicillin, and 100 $\mu\text{g}/\text{ml}$ streptomycin; Invitrogen; Thermo Fisher Scientific, Inc.) was added to achieve a total of 10 ml of 10 mM nominal concentration of selenium suspension and to also achieve a final ethanol concentration in the stock suspension of <1% (v/v) as a result of the progressive ethanol dilution throughout the preparation procedure.

Nominal selenium concentrations (μM) were calculated based on the total mass of Se^0 added relative to the final culture volume according to the equation ($m=C \times \text{MW} \times V$).

Reported concentrations represent nominal exposure concentrations based on total selenium mass, without the quantification of the dissolved or bioavailable fraction. No attempt was made to quantify the dissolved or bioavailable fraction of selenium in the culture medium. All preparation steps were performed under dim light conditions to minimize potential photochemical alterations. Tubes were protected from light using amber containers or aluminum foil wrapping. The vehicle (ethanol) and culture media were sterilized using a 0.22- μm filter prior to use. Due to the particulate nature of Se^0 , post-dispersion filtration was not performed to avoid the removal of suspended particles.

The five working concentrations of the compound were prepared fresh (5, 10, 25, 50 and 75 μM) by diluting the original 10 mM stock solution into complete culture medium immediately prior to treatment of the cells using the dilution formula ($C_1V_1=C_2V_2$). Prior to each dilution, the stock suspensions were vortexed for 5-10 sec to avoid sedimentation. Before diluting stocks in the culture wells, they were vortexed again to further minimize sedimentation and ensure even exposure. The compound selenium was added to cell treatments in 96-well plates as a pre-diluted working solution (total volume=100 μl). The desired final selenium in each well is shown in the results. The ethanol concentration in all treated wells was 0.1% v/v.

A solvent control group was used and received the same complete culture medium and conditions with ethanol at a final concentration $\leq 0.1\%$ (v/v) to assess the use of a solvent as a vehicle; this corresponds to the maximum solvent concentration present in the selenium-treated wells.

The stock suspensions were used within 2 h for long-term storage to avoid variations due to settling particles or oxidation. The methods for preparing and handling these stock suspensions were standardized and adapted from a published selenium cytotoxicology protocol (11) to produce reproducibility and accuracy in concentration.

Cell line and culture conditions. The human melanoma cell line, CHL-1, was obtained from the American Type Culture Collection (ATCC). After receiving the cells, they were grown, frozen in small portions, and then used in experiments at low passage numbers (passages 5-12) to reduce changes in their characteristics.

Dulbecco's modified Eagle's medium (DMEM; high glucose, 4.5 g/l glucose, manufactured by Invitrogen; Thermo Fisher Scientific, Inc.) was the basis for cell culture. The media contained 10% (v/v) heat-inactivated fetal bovine serum (FBS), 100 U/ml penicillin, and 100 $\mu\text{g}/\text{ml}$ streptomycin (all purchased from Invitrogen; Thermo Fisher Scientific, Inc.)

and were all incubated in a humidified 37°C incubator with 5% CO_2 and 95% air to maintain physiological pH. The media were exchanged every 48-72 h, and the cells were sub-cultured by trypsinization (0.25% trypsin-EDTA), reaching 70-80% confluency. Following trypsinization, the cells were neutralized in complete media (DMEM supplemented with 10% FBS, 100 U/ml penicillin, and 100 $\mu\text{g}/\text{ml}$ streptomycin; Invitrogen; Thermo Fisher Scientific, Inc.). The cells were centrifuged at 300 x g for 5 min at room temperature (25°C). Cells were subsequently reseeded to the appropriate density.

Regular observation of cell morphology using a contrast microscope to determine appropriate spindle-shaped adherent melanoma cell morphology. Cell viability (>95%) was assessed by trypan blue exclusion, and only viable cultures were used for experimental seeding. All culturing experiments were performed by using antibiotics (penicillin/streptomycin) to verify experimental accuracy, reduce biological variability, and prevent masking contamination. Mycoplasma testing was carried out with PCR-based detection assays and was confirmed to be negative throughout the experiments.

Cell viability assay (MTT assay). Cell viability was evaluated using the MTT assay as previously described (22,23), in which the viability of cells is assessed using a colorimetric method based upon reduction of the tetrazolium salt MTT by mitochondrial dehydrogenase activity of metabolically active cells to form insoluble purple formazan crystals. The amount of formazan produced is directly proportional to the number of viable cells.

For these experiments, CHL-1 melanoma cells were plated at 5×10^3 cells per well in 96-well flat-bottom plates in a final volume of 100 μl complete culture medium and allowed to attach overnight at 37°C and 5% CO_2 . The following day, the cells were subjected to increasing concentrations of Se^0 at nominal concentrations of 5, 10, 25, 50, and 75 μM for 24 or 48 h to determine the cytotoxicity based on both concentration and time. A vehicle control group containing 0.1% (v/v) ethanol was included with each data point. One-way ANOVA was used to compare the vehicle-treated group with the untreated control group. The untreated cells served as the negative controls (NC). Hydrogen peroxide (H_2O_2 ; Sigma-Aldrich; Merck KGaA; 75 μM) was used as a positive control to trigger cytotoxicity by oxidative stress. The concentration of H_2O_2 was determined based on a previous study (24) and initial optimization experiments; these investigations concluded the induction of measurable oxidative stress while limiting non-specific cell death.

Following each treatment, 10 μl of MTT solution (Sigma-Aldrich; Merck KGaA) (5 mg/ml in sterile PBS, yielding a final concentration of 0.5 mg/ml) were added to each well, thereby maintaining a 1:10 ratio of reagent to medium. After incubating the plates for 4 h at 37°C to produce formazan crystals, their culture media were removed using an aspirator without affecting the formazan crystals formed at the bottom of each well. A solubilizing agent was added at 100 μl (DMSO; Sigma-Aldrich; Merck KGaA) to each well to dissolve/integrate the formazan crystals. The plates were then agitated at room temperature for ~10-15 min. The absorbance of each specimen was determined using a microplate reader (BioTek Quant Plate Reader, BioTek; Agilent Technologies, Inc.) operating at 570 nm. The blank was subtracted from

the absorbance of the sample before calculating the relative viability of the cell. The calculation of cell viability was performed as follows: Cell viability (%) = $[(\text{OD sample} - \text{OD blank}) / (\text{OD control} - \text{OD blank})] \times 100$.

The blank was the media only supplemented with MTT reagent but containing no cells; the control was untreated cells used as the positive control (defined as 100% viability). The vehicle-treated cells did not exhibit a statistically significant difference in viability compared with the untreated controls ($P > 0.05$). Dose-response curves were generated using GraphPad Prism version 8.0.2 (Dotmatics), and IC_{50} values were determined by nonlinear regression using a four-parameter logistic (4PL) dose-response model (variable slope) in GraphPad Prism. The parameters of the model, including the top, bottom plateau, Hill slope and $\log \text{IC}_{50}$ values, were estimated by using least-squares fitting. Each treatment condition was tested in triplicate wells (technical replicates) within each independent experiment. Furthermore, the entire experiment was repeated three times (biological replicates). Data are presented as the mean \pm SEM ($n=3$). Exact P-values obtained from ANOVA are reported in the Results section, where applicable.

Comet assay. The alkaline comet assay was performed to assess DNA damage according to previously established protocols (25) with minor modifications. Before the comet assay analysis, CHL-1 melanoma cells were cultured and treated as described above. The cells were assigned to four experimental groups, as follows: i) The negative control (untreated cells); ii) positive control treated with $75 \mu\text{M}$ H_2O_2 (26); iii) Se^0 -treated cells ($7.50 \mu\text{M}$; corresponding to the IC_{50} value), and iv) cells treated with Se^0 ($7.50 \mu\text{M}$) combined with $75 \mu\text{M}$ H_2O_2 .

Cells were exposed to selenium ($7.50 \mu\text{M}$) for 30 min at 37°C . In the combined treatment group, H_2O_2 ($75 \mu\text{M}$) was co-administered during the same 30-min exposure period. Immediately following treatment, cell viability was assessed by trypan blue exclusion and confirmed to be $>85\%$, ensuring that DNA damage was not secondary to overt cytotoxicity. Cells were obtained via trypsinization followed by centrifugation at $300 \times g$ for 5 min at 4°C ; the resultant cell pellet was reconstituted in chilled PBS to an approximate density of 1×10^5 cells/ml. A total of $75 \mu\text{l}$ of 0.5% low-melting-point agarose (Sigma-Aldrich; Merck KGaA) was maintained at 37°C and mixed with $25 \mu\text{l}$ of cell suspension (immediately upon preparation). It was spread onto glass microscope slides (Thermo Fisher Scientific, Inc.) pre-coated with 1% normal-melting-point agarose (Sigma-Aldrich; Merck KGaA) and allowed to solidify at 4°C for 10 min. Preparation for the remaining procedures was carried out under low lighting conditions to minimize DNA damage.

Following at least 1 h of incubation at a temperature of 4°C in lysis buffer (all chemicals were purchased from Sigma-Aldrich; Merck KGaA) [2.5 M sodium chloride, 100 mM ethylene diaminetetraacetic acid (EDTA), 10 mM tris (hydroxymethyl) aminomethane (Tris); pH 10-10.5], the slides were removed from the lysis buffer to remove all cellular proteins and membranes. The slides were then placed into fresh alkaline electrophoresis buffer (chemicals from Sigma-Aldrich; Merck KGaA) [300 mM sodium hydroxide;

1 mM EDTA (pH >13)] for 20 min to allow DNA to unwind before performing the actual electrophoresis for 25 min at an applied voltage of 25 V ($\sim 0.8 \text{ V/cm}$), with a 300 mA current following a temperature of 4°C .

Following electrophoresis, the slides were neutralized in Tris buffer (Sigma-Aldrich; Merck KGaA) (0.4 M , pH 7.5) for a minimum of 5 min per wash (three total washes) before staining with ethidium bromide (Sigma-Aldrich; Merck KGaA) ($2 \mu\text{g/ml}$) for 5 min at room temperature in the dark. Comets were visualized using a fluorescence microscope (Olympus BX53; Olympus Corporation) at $\times 20$ magnification. DNA migration patterns were analyzed in a blinded manner. At least 100 randomly selected nuclei per slide were scored for each sample. Image acquisition was performed using a CCD camera system connected to Kinetic Imaging software. Comet parameters were quantified using Comet 6 image analysis software (Kinetic Imaging Ltd.), and images were exported as uncompressed BMP files. DNA damage was expressed as OTM and % tail DNA, which are sensitive indicators of oxidative DNA strand breaks (27).

Reverse transcription-quantitative PCR (RT-qPCR). The purity and concentration of total RNA were measured using a BioDrop™ Touch Duo spectrophotometer (BioDrop Ltd.) by determining the 260/280 ratio. cDNA synthesis was conducted according to the manufacturer's instructions using the iScript™ cDNA synthesis system (Bio-Rad Laboratories, Inc.). A total of three independent biological replicates for each condition were prepared, and triplicate (technical) qPCR reactions were carried out on each of the biological replicates to analyze them. A total of $20 \mu\text{l}$ of mixture consisted of $1 \mu\text{g}$ total RNA, $4 \mu\text{l}$ 5X iScript reaction mix, $1 \mu\text{l}$ iScript reverse transcriptase, and nuclease-free water to create cDNA. The Bio-Rad PTC-200 Peltier Thermal Cycler (Bio-Rad Laboratories Inc.) was used to perform reverse transcription. Reverse transcription was performed using the following conditions: 5 min at 25°C (priming), 20 min at 46°C (reverse transcription), 1 min at 95°C (inactivation), and a final hold of 10 min at 4°C . The synthesized cDNA samples were kept at -20°C .

qPCR was conducted using MicroAmp® Optical 8-Cap Strips in 96-Well Plates on a StepOnePlus Real-Time PCR Detection System (Applied Biosystems, Inc.). Each $20 \mu\text{l}$ reaction consisted of $10 \mu\text{l}$ SYBR®-Green Master Mix (Qiagen, Inc.), $2 \mu\text{l}$ primer, $4 \mu\text{l}$ nuclease-free water, and $4 \mu\text{l}$ diluted cDNA. The cycling conditions were as follows: An initial denaturation at 95°C for 10 min was followed by 40 cycles at 95°C for 15 sec and 60°C for 1 min; the melt curve (i.e., 95°C for 15 sec and 60°C for 15 sec, followed by 95°C for 15 sec) followed by melt curve analysis confirmed specificity and that each primer pair amplified a single specific product. Each run included no-template controls and no-reverse-transcription controls (no reverse transcription controls).

Relative gene expression was calculated using the $2^{-\Delta\Delta\text{C}_q}$ method (28). β -actin was used as the internal reference gene, and its expression was confirmed to be stable under the tested conditions (29). Primer efficiencies were determined from 5-point serial dilutions of cDNA and were within the acceptable range of 90-110% (slopes -3.1 to -3.6 , $R^2 > 0.99$). The primer sequences are listed in Table I (30-34). All data-sets were examined for data entry accuracy prior to analysis.

Table I. Primer sequences used for RT-qPCR analysis.

Genes	Primer sequence (5' to 3')	(Refs.)
<i>p53</i>	F: 5'-CCTCAGCATCTTATCCGAGTGG-3' R: 5'-TGGATGGTGGTACAGTCAGAGC-3'	(30)
<i>p21</i>	F: 5'-AAGTCAGTTCCTTGTGGAGCC-3' R: 5'-GGTTCTGACGGACATCCCCA-3'	(31)
<i>Caspase-3</i>	F: 5'-ATGGAAGCGAATCAATGGA-3' R: 5'-TGTACCAGACCGAGATGTC-3'	(32)
<i>Bcl-2</i>	F: 5'-GGATCCAGGATAACGGAGGC-3' R: 5'-CCAGATAGGCACCCAGGGT-3'	(33)
<i>β-actin/ACTB</i>	F: 5'-CCTGGCACCCAGCACAAAT-3' R: 5'-GCCGATCCACACGGAGTACT-3'	(34)

RT-qPCR, reverse transcription-quantitative PCR; F, forward; R, reverse. All primer sequences were adopted from the indicated previously published studies.

Experimental data are presented as the mean ± SEM derived from at least three independent biological experiments (n=3), each performed with technical replicates as described above.

Statistical analyses. All datasets were conducted using GraphPad Prism version 8.0.2 (Dotmatics). The distribution was assessed using the Shapiro-Wilk test before performing parametric analyses. For comparisons among multiple groups, one-way ANOVA was applied, followed by Tukey's post hoc test for pairwise multiple comparisons. For the MTT assay, statistical analyses were performed separately for the 24- and 48-h treatment time points. For RT-qPCR analysis, as the relative expression values derived from the $2^{-\Delta\Delta Cq}$ method are log-normally distributed, fold-change data were \log_2 -transformed before statistical analysis to approximate normal distribution and satisfy the assumptions required for parametric ANOVA testing. Statistical comparisons between experimental groups were performed using one-way ANOVA followed by Tukey's post hoc test for multiple comparisons. A value of $P < 0.05$ was considered to indicate a statistically significant difference. Fold-change values are presented in the figures for biological interpretation. No data points were excluded from the analysis. All statistical tests were two-tailed.

Results

Cytotoxic effects of selenium on CHL-1 melanoma cells. Cell viability was assessed using the MTT assay following 24 and 48 h of exposure to increasing concentrations of Se^0 (5-75 μM). Exposure to selenium induced a concentration- and time-dependent reduction in CHL-1 cell viability (Fig. 1). The vehicle-treated cells (ethanol $\leq 0.1\%$ v/v) did not exhibit a statistically significant difference in viability compared with untreated control cells (one-way ANOVA, $P > 0.05$) and were therefore considered equivalent to baseline conditions.

At 24 h following treatment with selenium, the viability of the CHL-1 cells decreased in a concentration-dependent manner. In the absence of selenium, the mean percentage of viable cells was $100 \pm 0.01\%$; however, the cells treated with 5, 10, 25, 50, and 75 μM selenium exhibited a viability of

55 ± 0.23 , 45 ± 0.45 , 38 ± 0.56 , 25 ± 0.35 , and $18 \pm 0.13\%$, respectively (n=3). At 48 h following treatment with selenium, even lower percentages of viable cells were noted, with the mean levels being 52 ± 0.03 , 43 ± 0.49 , 34 ± 0.66 , 22 ± 0.35 and $13 \pm 0.06\%$, respectively, as compared to the aforementioned mean percentages.

The viability of the CHL-1 cells exposed to 75 μM (positive oxidative stress control) H_2O_2 decreased to $75 \pm 0.04\%$ at 24 h and $78 \pm 0.15\%$ at 48 h following treatment (indicated by the isolated red data points in Fig. 1). A statistically significant treatment effect was determined using one-way ANOVA at both time points ($P < 0.05$). Non-linear regression analysis of the 48-h dose-response curve (plotted in Fig. 1) indicated an IC50 value of 7.50 μM .

Selenium enhances DNA strand breakage in CHL-1 cells. DNA strand breaks were quantified using the alkaline comet assay and expressed as both % tail DNA and OTM, as demonstrated below and in Figs. 2-4.

Percentage of tail DNA (% tail DNA). CHL-1 cells originally were able to achieve low levels of DNA damage with only a mean % tail DNA of 27.90 ± 1.19 when left untreated. Following exposure of these cells to 75 μM H_2O_2 , the amount of DNA fragmentation increased significantly from baseline, with a mean % tail DNA of 37.77 ± 1.05 . Conversely, when the cells were treated with 7.50 μM selenium alone, this treatment increased tail DNA (38.70 ± 0.57). Furthermore, the highest level of DNA damage occurred in cells treated concurrently with selenium and H_2O_2 (44.67 ± 1.13).

Analysis using one-way ANOVA demonstrated that each treatment had a significant effect on % tail DNA [$F(3,8) = 45.95$, $P = 2.18 \times 10^{-5}$]. In addition, Tukey's post hoc analysis revealed that each treatment with H_2O_2 and selenium alone, as well as the concurrent treatment with H_2O_2 and selenium, produced significantly more DNA damage compared with the untreated CHL-1 cells ($P < 0.001$). No significant difference was observed between the groups treated with H_2O_2 and selenium ($P > 0.05$).

Improved pairwise analysis indicated that concurrent treatment with selenium and H_2O_2 resulted in more DNA

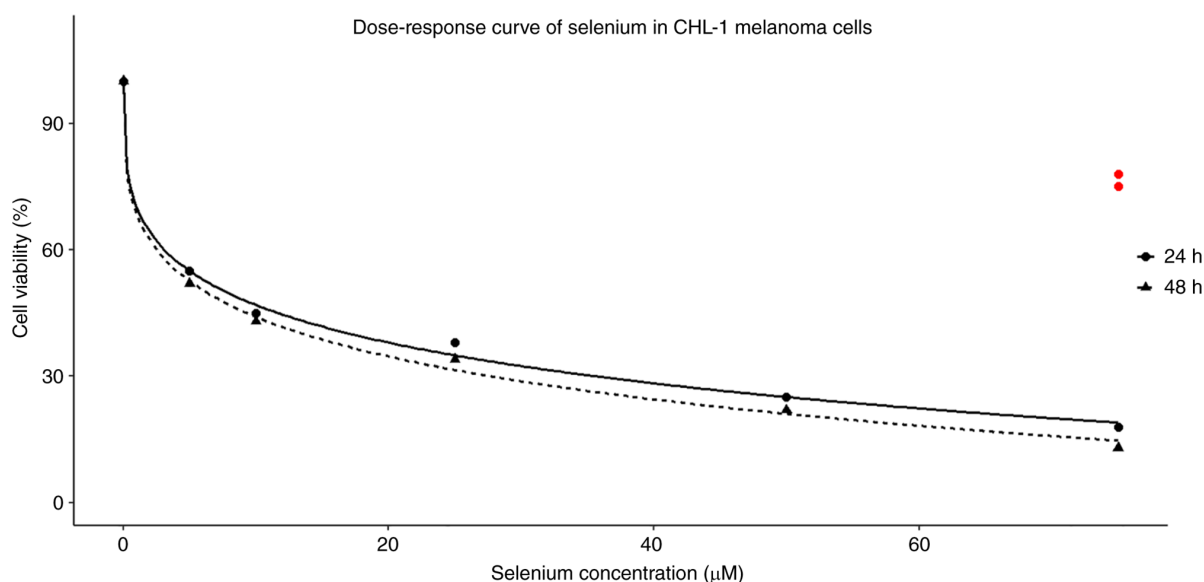


Figure 1. Cytotoxic effects of selenium on the viability of CHL-1 melanoma cells assessed using MTT assay. MTT was utilized to determine the concentration- and time-dependent effects of curative cancer treatment using selenium, a natural supplement with anti-cancer properties. To perform this experiment, cells were treated with increasing concentrations of elemental selenium (5 to 75 μM) during both the 24 and 48 h of the trial, with resulting cell viability reported as a percentage of the time-matched control. Selenium treatment resulted in decreased cell viability with increasing concentrations and varying durations of treatment. Hydrogen peroxide at 75 μM was used as an oxidation control for the occurrence of cytotoxicity due to oxidative stress (represented by the red data points on the graph); results of the tests are expressed as mean values (mean \pm SEM, $n=3$) from a total of 3 separate experiments ($n=3$). The calculated IC50 value derived from the 48-h dose-response curve is 7.50 μM .

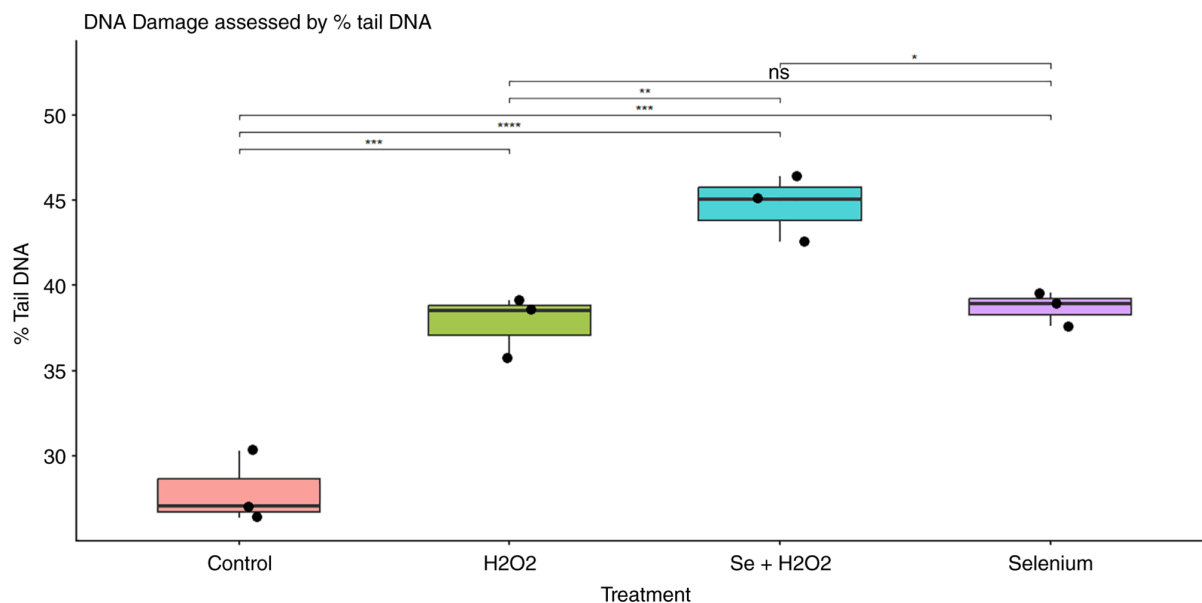


Figure 2. The ability of selenium and H_2O_2 to induce DNA damage was evaluated using the OTM. The extent of DNA fragmentation from selenium-treated CHL-1 melanoma cells was assessed with the alkaline comet assay, and DNA strand breakage was quantified using the OTM. Cells were not treated, treated with selenium at its IC50 (7.50 μM), treated with 75 μM H_2O_2 (positive control), or treated with both selenium and 75 μM H_2O_2 . DNA fragmentation in untreated cells was significantly higher in selenium compared to those that did not receive any treatment, thus indicating that selenium is a genotoxic inducing agent, which produced more DNA fragmentation than H_2O_2 alone. The use of H_2O_2 in addition to selenium resulted in higher OTM values than both treatments alone; therefore, the combination of selenium and hydrogen peroxide produced more oxidative DNA damage than either treatment alone. The data are expressed as the mean \pm SEM for the three independent experiments, using a one-way ANOVA with Tukey's post hoc to determine significance ($^*P<0.05$, $^{**}P<0.01$, $^{***}P<0.001$ and $^{****}P<0.0001$; ns, not significant). OTM, olive tail moment; H_2O_2 , hydrogen peroxide; Se, selenium.

damage than either treatment with H_2O_2 ($P<0.01$) or with selenium ($P<0.05$) alone. Thus, each treatment led to increased levels of DNA damage; however, the degree of DNA fragmentation was greatest when evaluated under combined oxidative conditions using both selenium and H_2O_2 .

OTM. The average OTM in the untreated CHL-1 cells was 7.61 ± 0.41 , indicating minimal baseline DNA damage. Exposure to H_2O_2 (75 μM) significantly increased DNA damage, resulting in an average OTM value of 15.47 ± 0.60 . Cells treated with selenium alone at 7.50 μM also exhibited increased DNA

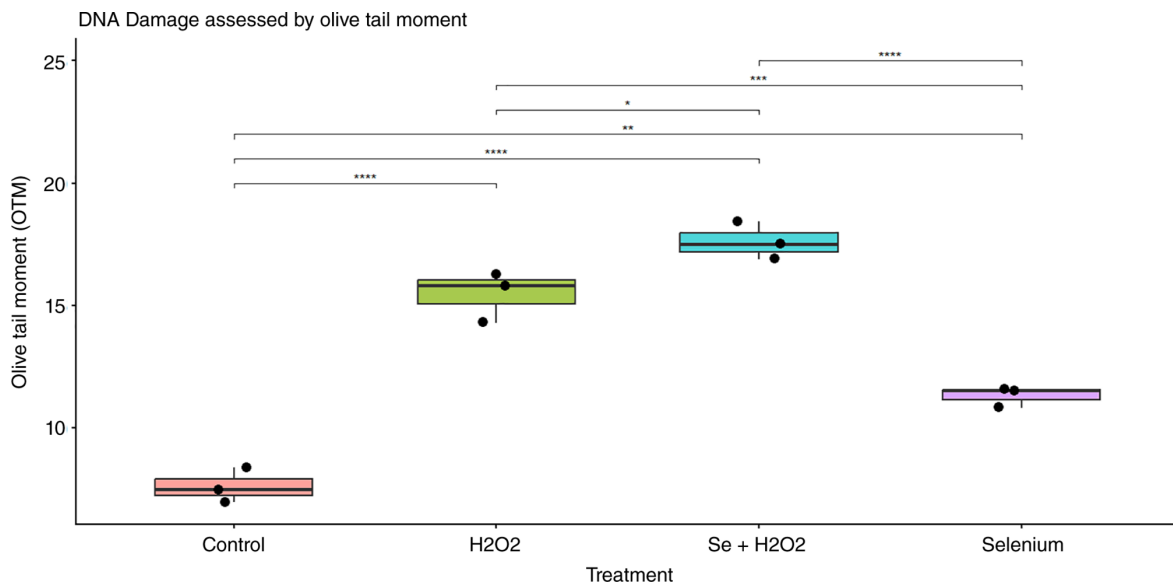


Figure 3. Selenium and selenium plus H₂O₂ induce significant DNA damage as evidenced by the amount of tail DNA percent, relative to the amount of tail DNA percent in CHL-1 melanoma cells treated with selenium (7.50 μM), H₂O₂ (75 μM), and both selenium and H₂O₂ concurrently. The untreated controls had very limited amounts of % tail DNA, but selenium treatment resulted in a marked increase in tail DNA percent, confirming that selenium is a genotoxicant. Concurrent treatment with selenium and H₂O₂ resulted in a significantly higher tail DNA percentage than either treatment alone and demonstrated an increased sensitivity of the cells to oxidative DNA damage. Data are presented as the mean ± SEM of three independent experiments. Statistical analysis was performed by one-way ANOVA with Tukey's post hoc test; (*P<0.05, **P<0.01, ***P<0.001 and ****P<0.0001). H₂O₂, hydrogen peroxide; Se, selenium.

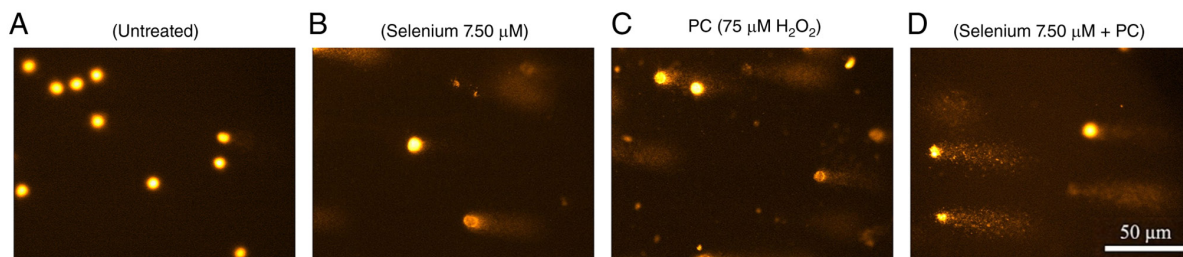


Figure 4. Representative comet assay analysis illustrating DNA damage in CHL-1 melanoma cells under different treatment conditions. Representative fluorescence micrographs of CHL-1 cells stained with ethidium bromide following alkaline comet assay. Cells were treated with (A) untreated control, (B) selenium (7.50 μM), (C) H₂O₂ (75 μM; positive control), and (D) selenium (7.50 μM) combined with H₂O₂ (75 μM). Images were acquired under identical imaging conditions using a 20X objective. Untreated cells exhibited intact nuclei with minimal DNA migration. Selenium-treated cells showed moderate DNA fragmentation. Hydrogen peroxide treatment resulted in pronounced comet tail formation, indicating increased DNA strand breaks. The combined selenium and hydrogen peroxide treatment produced the most extensive DNA damage, with marked tail elongation and increased DNA dispersion. These qualitative observations are consistent with the quantitative analysis of % tail DNA and olive tail moment, demonstrating a progressive increase in DNA damage across treatment groups. H₂O₂, hydrogen peroxide; PC, positive control. Scale bar, 50 μm.

damage, with an average OTM value of 11.30±0.24. Combined treatment with selenium and H₂O₂ produced the highest level of DNA damage, with an average OTM value of 17.62±0.45. Based on one-way ANOVA analysis, the treatment conditions had a highly significant effect on OTM values in CHL-1 cells [F(3,8)=98.46, P=1.18x10⁻⁶].

Tukey's multiple comparison tests revealed that H₂O₂, selenium alone, and combined treatment with selenium + H₂O₂ all produced significantly higher OTM values compared with the untreated CHL-1 cells (P<0.01 for all comparisons). In addition, significant differences were observed between the H₂O₂ and selenium treatment groups (P<0.01). Pairwise comparisons further indicated that combined treatment with selenium + H₂O₂ produced significantly greater DNA damage compared with H₂O₂ alone (P<0.05) and selenium alone (P<0.01). Representative comet images (Fig. 4) qualitatively

supported the quantitative findings, illustrating progressively increased DNA damage across treatment conditions.

Effect of selenium and H₂O₂ on the expression of apoptosis-related genes in CHL-1 cells. Log₂-transformed fold change values were used to compare the experimental groups. The relative mRNA expression levels of *p53*, *p21*, *caspase-3*, and *Bcl-2* were assessed using RT-qPCR, normalized against the internal reference gene, β-actin, and presented as a ratio relative to untreated control cells, which were assigned a value of 1.0 (Fig. 5).

Exposure to H₂O₂ increased *p53* expression by 4.85-fold relative to the control; selenium (7.50 μM) increased *p53* expression by 3.47-fold relative to the control. Following exposure to H₂O₂, the expression of the cyclin-dependent kinase inhibitor, *p21*, was measured as ~3.45-fold that of the

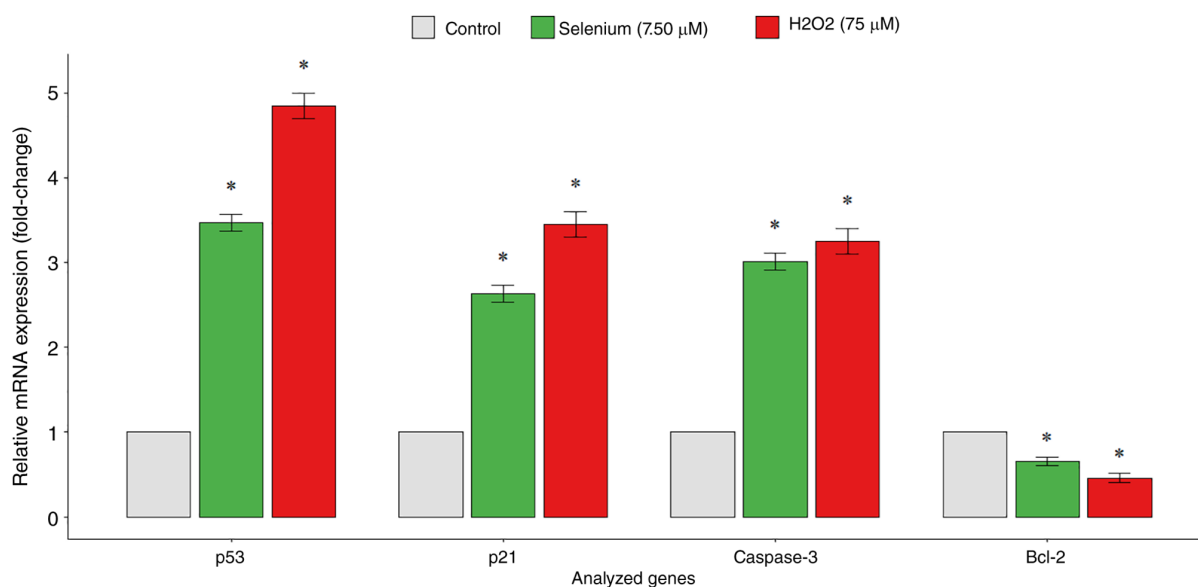


Figure 5. The mRNA expression levels of genes in the CHL-1 melanoma cells following exposure to 7.5 μM selenium or 75 μM of H₂O₂ determined using reverse transcription-quantitative PCR. The genes analyzed involved *p53* (as the tumor suppressor gene and DNA damage sensor that activates stress response signals), *p21/CDKN1A* (a cyclin-dependent kinase inhibitor to *p53* that promotes cell cycle arrest at the G1/S checkpoint), *caspase-3* (an executing protease involved with final stages of intrinsic apoptosis), and *Bcl-2* (an anti-apoptotic mitochondrial protein that inhibits protease to activate caspases and maintains the integrity of mitochondrial membranes). All expression level data were normalized relative to the reference gene, β-actin and reported as the relative fold change from control cells (set as 1.0). Statistical significance compared to the untreated control is indicated by asterisks (*P<0.05). Data were analyzed using one-way ANOVA followed by Tukey's post hoc test, where all treatment groups were statistically different from each other based on a log₂ transformation of raw data.

control. In the selenium-treated cells, *p21* expression was ~2.63-fold that of the control. Statistical analysis (ANOVA followed by Tukey's test) demonstrated a statistically significant treatment-dependent difference in the expression levels of both *p53* and *p21* based on treatment (P<0.05) (Fig. 5).

The mRNA expression of *caspase-3* was markedly increased in both treatment groups, with levels in the H₂O₂ group being 3.25-fold those of the controls and 3.01-fold those of controls in the selenium group. ANOVA followed by Tukey's test determined that the treatments had a significant effect on the *caspase-3* expression level (P<0.05) (Fig. 5).

The expression of *Bcl-2* (an anti-apoptotic gene) significantly decreased following each treatment condition. With respect to *Bcl-2* expression, exposure to H₂O₂ resulted in *Bcl-2* expression being reduced to 0.46-fold compared to the untreated controls; treatment with selenium reduced *Bcl-2* expression to 0.65-fold (P<0.05) (Fig. 5).

Both selenium and oxidative stress exposure result in a coordinated upregulation of pro-apoptotic and cell cycle regulatory transcripts (*p53*, *p21*, and *caspase-3*), with the downregulation of the anti-apoptotic gene, *Bcl-2*. This transcriptional profile corresponds with the increased DNA strand breakage observed in comet assay analyses, thereby suggesting a coordinated, treatment-dependent cellular stress response within CHL-1 cells (Fig. 5).

Discussion

Melanoma, an aggressive type of cancer, is known for its ability to adapt to changes in oxidation and reduction (redox) conditions, its metabolic flexibility, and its resistance to treatment (35,36). The present study aimed to systematically determine if the cell-killing effects of selenium in CHL-1 melanoma cells are

directly related to oxidative DNA damage and the coordinated changes in the expression of genes in the *p53* pathway. The present study combined tests that measure cell survival, a comet assay to quantify DNA damage, and *p53*, *p21*, *caspase-3*, and *Bcl-2* expression, all within the same experiment. To date, few studies (37,38) have simultaneously considered how selenium affects cell death, quantitatively assessed DNA damage, and analyzed the expression of genes in the *p53* pathway within the same melanoma model. In addition, using external H₂O₂ as a controlled source of oxidative stress strengthens this systematic approach by functionally confirming the ability of selenium to enhance the sensitivity of the cells' redox changes under conditions that mimic the stress of a tumor environment.

The results of the MTT assay indicated that selenium significantly decreased the viability of CHL-1 cells in both a concentration- and time-dependent manner (IC₅₀, 7.50 μM; Fig. 1). In addition, the results are consistent with previous research that demonstrated the increased sensitivity of melanoma cells to redox-disrupting compounds due to their high basal levels of ROS and limited ability to further regulate them during oxidative stress (39,40). Chronic levels of ROS can support the proliferation and survival of melanoma cells through moderate amounts of ROS signaling. When excessive ROS overwhelm antioxidant defenses, cellular damage becomes irreversible, leading to cell death. The higher level of cytotoxicity at 48 h compared to 24 h of selenium exposure observed herein also indicates that selenium-induced oxidative stress may have a cumulative or delayed effect on the ability of the cells to mount adaptive antioxidant responses (41). Research supports this time-dependent pattern, demonstrating that selenium-induced cytotoxicity is associated with the generation of intracellular ROS rather than through acute oxidative stress (42). The results of decreased viability of cells exposed to selenium were similar

to the effects of exposure to H_2O_2 , supporting the role of selenium as a redox-modulating agent in melanoma cells. ROS are highly reactive towards several cellular macromolecules, but one of the most sensitive targets is DNA; therefore, the oxidative stress-induced damage to DNA is one of the critical factors that determines the fate of a cell (43).

The IC_{50} dose level and treatment with selenium significantly increased OTM and % tail DNA, suggesting the induction of significant DNA strand breaks and alkali-labile sites consistent with oxidative DNA damage. The present study presents integrated evidence linking selenium-induced oxidative DNA damage with the coordinated activation of p53-dependent apoptotic signaling in CHL-1 melanoma cells. These findings are in agreement with those of previous studies that reported the ability of selenium to induce both single- and double-(two-ended) strand breaks in cancer cells due to oxidative damage to DNA (44,45). The presence of such damage activates a biological pathway known as the DDR. The response of a cell to the severity of an insult will depend on the activation of the DDR pathway, including cell cycle arrest, repair of the damage, or apoptosis (46).

Melanoma is an aggressive type of skin cancer that has a high incidence of mutations related to the repair of DNA damage and is often characterized by alterations to DDR pathways. Increased DNA damage caused by excessive oxidative stress will induce a shift in the apoptotic response from cell survival or repair to cell death. In the present study, when melanoma cell lines were treated with both selenium and H_2O_2 , they exhibited a substantial increase in DNA damage compared to treatments with either agent alone. The addition of H_2O_2 into the study provided functional evidence of the redox-sensitizing properties of selenium. When selenium and H_2O_2 were used in combination, it appeared that selenium rendered melanoma cells less tolerant to oxidative stress from an outside source and therefore increased the amount of genotoxic stress experienced by these cells from an outside source of oxidative stress. In summary, these findings describe the ability of selenium to be a redox sensitizer by decreasing the oxidative stress tolerance threshold of melanoma cells and increasing the amount of genotoxic stress that these cells experience from outside sources of oxidative stress. Thus, the data indicate that selenium lowers the redox resistance of melanoma cells, rendering them more sensitive to oxidative stress (47). In addition, emerging evidence suggests that melanoma cells may also be susceptible to other metal ion-induced cell death mechanisms, such as cuproptosis, which occurs with the presence of copper, causing mitochondrial stress and metabolic dysfunction. Although different from the mechanism of redox imbalance of selenium, this evidence supports the broader notion that disrupting trace element-related metabolic and redox-dependent mechanisms may be a promising treatment strategy for melanoma (48).

As a result of previous studies, there are multiple strategies that use redox-active agents to increase the sensitivity of cancer cells to oxidative stress; for example, by breaking down the normal buffering capacity of antioxidant systems. This is crucial as it allows for an understanding of how the selenium-mediated modulation of redox can produce an increase in the effectiveness of oxidative and targeted therapies and suggests that future research using combination

models is warranted. These findings have clinical significance outside of the *in vitro* models, due to their implications for resistance to therapy in patients with melanoma. Specifically, targeted therapies that inhibit BRAF and MEK have been associated with the development of adaptive metabolic reprogramming and the incorporation of enhanced antioxidant defense systems, both of which present significant clinical problems (49-51). Melanoma cells that develop resistance to targeted therapies can alter their redox homeostasis in such a manner as to provide mitigation against the accrual of excess ROS, which improves survival and tolerance to these therapeutics. In this regard, the ability of selenium to disrupt redox balance within cells and amplify DNA oxidative damage may provide the mechanistic basis for shifting the oxidative tolerance level of resistant melanoma phenotypes. Although the present study did not directly evaluate drug-resistant models, the observed redox sensitization and coordinated activation of p53-dependent apoptotic signaling provide a conceptual framework through which selenium could potentially enhance responsiveness to targeted therapies. Future investigations using BRAF inhibitor-resistant melanoma cell lines or combination treatment models are warranted in order to determine whether selenium-mediated redox modulation can overcome clinically relevant resistance mechanisms (52).

The identification of key genes that regulate apoptosis and the cell cycle was performed to identify the mechanisms whereby selenium causes molecular changes in DNA. Selenium was shown to increase the levels of expression of *p53*, *p21*, and *caspase-3*, while decreasing the levels of expression of the anti-apoptotic gene, *Bcl-2*, in the selenium-treated cells compared to the controls. This increase in the expression of the genes identified is indicative of p53-mediated cell cycle arrest and the initiation of intrinsic apoptotic pathways. p53 functions as a 'central' regulator (sensor) of genotoxic stress via the promotion of transcriptional programs that establish the fate of a cell in response to DNA damage (53). Herein, the increase in the expression of *p21* observed in the selenium-treated cells indicates that p53 is mediating the enforcement of cell cycle arrest at the G1/S transition so that the integrity of the DNA can be checked (54). When the damage to the DNA is beyond the ability of the cell to repair itself, *p53* may redirect its efforts from inducing cell cycle arrest to inducing apoptosis in the cell by activating the expression of pro-apoptotic factors, such as *caspase-3*, and inhibiting the expression of anti-apoptotic genes such as *Bcl-2*. The downregulation of *Bcl-2* expression observed in selenium-treated cells is particularly important in the context of melanoma, since *Bcl-2* overexpression is a well-established means by which melanoma cells can avoid undergoing apoptosis or lose the ability to respond to chemotherapy (55). By decreasing the expression of *Bcl-2*, selenium may permit a decrease in the threshold for apoptosis and consequently enhance mitochondrial outer membrane permeabilization, resulting in increased caspase-dependent cell death (56). Similar mitochondrial apoptotic shifts mediated by modulation of *Bcl-2* family members have been reported for other bioactive compounds, including plant-derived molecules that induce apoptosis through alteration of the BAX/BCL-2 ratio. These findings support the biological plausibility of selenium-induced mitochondrial apoptotic priming in the present study (57).

Exposure to H₂O₂ caused the same gene expression pattern, which confirmed that oxidative stress alone is sufficient to initiate apoptotic signaling in CHL-1 cells. These findings suggest that selenium-induced cytotoxicity occurs through redox-dependent mechanisms. Selenium-induced redox perturbation may interconnect with one or other redox-sensitive signaling systems involved in melanoma development and chemotherapy resistance, even though the present study searched for the p53-dependent apoptotic axis as the main focus.

The generation of ROS affects the signaling properties of the PI3K/Akt signaling pathway through the oxidative inactivation of the phosphatase tumor suppressor, PTEN, which, when functioning, promotes death-signaling via p53 in the presence of low levels of oxidative stress. When there are increased levels of ROS, this leads to the decreased phosphorylation of Akt, promoting death signaling via apoptosis (58,59).

Sustained oxidative stress affects the signaling properties of the NRF2 antioxidant response pathway, which is the master regulator of redox homeostasis and serves to regulate the metabolic adaptation of melanoma cells to chemotherapy and resistance to chemotherapy. NRF2 signaling dysregulation associated with sustained oxidative stress may compromise the cellular antioxidant buffering system and thereby sensitize melanoma cells to additional oxidative stress (60,61).

In addition, high levels of ROS can result in increased lipid peroxidation, thereby increasing susceptibility to a regulated form of cell death termed ferroptosis, suggesting that selenium-induced redox imbalance may affect several types of regulated cell death, separate from classical p53-dependent apoptosis (62,63). Although the present study did not examine these pathways, their well-established redox sensitivity suggests that they present an explanation as to how selenium-induced oxidative stress could lead to a variety of melanoma signaling pathways (40,42,52).

The results from the present study support an integrated mechanistic model that indicates selenium exposure is associated with i) an imbalance in redox homeostasis; ii) oxidative DNA damage; and iii) the induction of the p53 signaling pathway. This overall process provides support for the mechanistic framework proposed in the introduction and demonstrates that selenium may lead to enhanced oxidation (and death) of melanoma cells. However, there has yet to be direct evidence of the transcriptional activation of p53 in response to combined treatment with selenium and H₂O₂.

The present study included multiple endpoints (cytotoxicity, genotoxicity, and gene expression), rather than evaluating a single endpoint, which was the case for previous studies (64-66). Thus, the data present a more comprehensive understanding of how selenium exerts cytotoxicity against melanoma cells. In addition, the present study demonstrated that selenium enhanced oxidative DNA damage in a manner that was dependent on exogenous sources of oxidative stress. Finally, these findings suggest that redox-based combination approaches can circumvent resistance mechanisms of melanoma (67-69). Therefore, future studies are required to include the validation of functional protein expression (phosphorylated p53 and cleaved caspase-3) along with the measurement of intracellular ROS to elucidate the mechanisms by which selenium causes cell death or impaired function.

Normal selenium levels at physiological levels are 0.8-1.5 μ M (70-120 μ g/l), based on individual dietary and geographical differences. This is sufficient for maximum performance and the activity of all the major selenoproteins (e.g., glutathione peroxidases and thioredoxin reductases), which are critical to maintaining redox balance in the body. Provided that physiological selenium levels are greater than those in the present study, additional amounts of selenium do not increase activity proportionally, and if selenium levels remain above physiological levels for long periods of time, the potential for selenium toxicity increases (70).

For the present study, concentrations should be viewed as pharmacological rather than nutritional; the maximum amounts of selenium obtained through dietary sources will not present sustained selenium levels above physiological levels. Therefore, long-term elevations lead to unintentional side-effects such as gastrointestinal complaints, brittle nails and hair, and in extreme cases, selenosis. While the amounts of selenium used in the present *in vitro* study are effective for elucidating cytotoxic mechanisms caused by oxidative stress in melanoma cells, further investigations on optimal dosing and targeted delivery methods are warranted before applying the results to individuals (71).

There are some critical limitations in the present study as well, despite its benefits. The first limitation is that one melanoma cell line (i.e., CHL-1) was used for the present study; however, this cell line is known to be an established redox-adapted model of melanoma (72,73). There are a number of genetic and metabolic differences between subtypes of melanoma, and the mutational makeup of a cell may affect its sensitivity to selenium due to how the cell regulates redox and undergoes apoptosis (51,74). In order to determine whether or not the findings of the present study can be generalized across melanomas, it would be necessary to validate these findings with multiple melanoma cell lines capable of being characterized into different molecular profiles. Future studies are required to include different mutational backgrounds in their cell lines, including a cell line that has a BRAF mutation and a cell line that has an NRAS mutation, to determine whether the redox-sensitization properties of selenium also hold for these genetically diverse subtypes of melanoma. Additional comparative analyses will help provide further evidence that the data presented in the present study are generalizable and relevant to the treatment of melanoma.

Another limitation of the present study is evaluating differences in sensitivity between malignant (tumor) and non-malignant cells using a normal human melanocyte population. Therefore, the selective vulnerability of melanoma cells to the toxicity of selenium is due to a difference in redox sensitivity between the malignant and non-malignant cells (19,20). Further research is thus required with the inclusion of a normal human melanocyte control group to present the necessary information to determine the therapeutic selectivity of selenium therapy, as well as the safety margins of selenium therapy. The absence of a normal human melanocyte control group will prevent the ability to definitively determine whether or not malignant and non-malignant melanocytes differ in their redox sensitivity. Establishing a difference in sensitivity will be critical for defining the therapeutic window of selenium and evaluating the potential for off-target toxicity (75).

The limits of the present study not only affect antioxidant activity but also present a critical perspective on another major issue, selenium speciation. The form of selenium will affect its biological action, since there are a number of different chemical forms (i.e., sodium selenite and selenomethionine), and their biological actions differ significantly in terms of their pharmacokinetic, pharmacodynamic, or redox-modulating actions (76). Additionally, elemental selenium has very little in common with either soluble inorganic or organic forms of selenium, making it essential, in terms of providing full and true extrapolations from the present findings into other selenium forms, to perform a systematic and direct comparative analysis across the various selenium forms to make rational therapeutic choices.

In some cases, inorganic forms can generate more free radical damage than organic forms can, as they create free radicals directly from their reaction with the oxygen in the surrounding environment. By contrast, the organic forms of selenium may primarily function as antioxidant agents via their incorporation into selenoproteins that serve to regulate oxidative stress (43). Selenium nanoparticles are also considered unique regarding their biological potential due to the altered kinetics of cellular uptake and potentially enhanced therapeutic indices observed in preclinical studies using cancer (77). These differences in how selenium functions in the body could result in differences in the dynamics and the levels of reactive oxygen species generated in cells, the levels of damage to the DNA, the amount of activation of apoptotic signaling, and the overall cytotoxic potential of different selenium species (78). Therefore, to develop an adequate understanding of the relationship between the structure and activity of selenium species in the treatment of melanoma, it is critical to conduct systematic and comparative evaluations of the outcomes of treatment with different selenium species *in vitro* and *in vivo* (79,80).

Another limitation of the present study is that transcriptional profiles of select apoptosis-related genes (*p53*, *p21*, *caspase-3*, and *Bcl-2*) were not evaluated in the selenium + H₂O₂ treatment group. The comet assay provided clear evidence of markedly increased DNA damage under combination redox stress conditions; however, the downstream activation status of the p53-dependent apoptotic pathway was never assessed in this group. While there is a biologically plausible association between increased levels of genotoxicity and subsequent enhancement of p53-mediated signaling, this type of mechanistic association was not evaluated at the transcriptional level using experimental methods. Thus, future studies including both gene and protein level studies (including phosphorylated p53, cleaved caspase-3, and mitochondrial apoptotic indicators) under combined oxidative stress will provide a more detailed understanding of whether selenium redox-mediated effects on apoptosis correspond to increased levels of apoptosis. On the whole, however, the results revealed the potential role of selenium as a redox-modulating chemoresistant agent in melanoma.

Future studies are based on the concept of selenium as a redox sensitizer by confirming previous studies performed *in vitro* by repeating these studies in an *in vivo* model, such as a melanoma xenograft or syngeneic model, to determine whether selenium enhances the tumor response to its own oxidative stress or to standard-of-care treatment. In addition to this, it is anticipated that combining selenium with targeted drugs (i.e.,

BRAF or MEK inhibitors) or agents that induce regulated cell death (e.g., apoptosis and ferroptosis) would allow researchers to gain insight into whether selenium-induced ROS elevation enhances the apoptotic priming of melanoma models resistant to targeted therapy. These experiments will present insight into whether the selenium-induced dysregulation of redox homeostasis can delay or eliminate adaptive resistance to treatment regimens. Furthermore, researchers need to be meticulous in measuring the systemic toxicity of these compounds to each model, as well as determining whether there is a difference when comparing the toxicity to both tumor and normal melanocytes, to determine the therapeutic window of redox-modulating agents (81). These proposed experiments will present a transition zone between the experimental design of all the mechanistic *in vitro* assays and the possible clinical use of these compounds/therapies (82).

In conclusion, the present study demonstrates that selenium causes considerable cytotoxic effects to CHL-1 melanoma cells through oxidative DNA damage and through the activation of p53-dependent apoptotic signaling cascades. As a result of exploiting the redox susceptibility of melanoma cells, selenium exposure disrupts intracellular redox homeostasis, leads to the accumulation of DNA damage, and induces apoptosis. These are significant mechanistic insights into selenium-mediated redox disruption in melanoma cells and serve to support additional investigative studies to determine the biological significance of selenium as a redox-disrupting agent in more complex experimental systems.

In conclusion, selenium was demonstrated to induce cytotoxicity in CHL-1 human melanoma cells via redox-mediated mechanisms in the present study. By concentration and time (IC₅₀=7.50 μM), selenium decreased cell viability and also resulted in increased levels of oxidative DNA damage, indicated by an increase in the number of cells exhibiting an OTM and/or the amount of % tail DNA. Furthermore, toxicity was exacerbated in the presence of H₂O₂ when combined with selenium under oxidative conditions, indicating that redox sensitization was mediated by oxidative stress.

At the molecular level, selenium increased the expression of *p53*, *p21*, and caspase-3 and decreased the expression of *Bcl-2*, suggesting that *p53* initiates both the intrinsic pathway of apoptosis and cell cycle arrest for cells undergoing apoptosis. Collectively, these changes suggest that the mechanism of action of selenium is to disrupt the redox homeostasis of melanoma cells, driving them beyond their oxidative tolerance threshold and inducing the initiation of apoptosis.

While the results of the present study provide evidence supporting the potential for selenium to be a redox modulating agent, increasing susceptibility to oxidative stress in melanoma cells, further *in vivo* studies are required to further elucidate the mechanisms of action of selenium for the purpose of establishing the translational relevance of these observations.

Acknowledgments

Not applicable.

Funding

No funding was received.

Availability of data and materials

The data generated in the present study may be requested from the corresponding author.

Authors' contributions

All authors (MA, BS and MMW) conceptualized the study, analyzed the data, wrote the first draft of the manuscript, revised and analyzed the data, assisted with graphical work, assisted with data collection, and created the figures. MA and MMW confirm the authenticity of all the raw data. All authors have read and agreed to the published version of the manuscript.

Ethics approval and consent to participate

Not applicable.

Patient consent for publication

Not applicable.

Competing interests

The authors declare that they have no competing interests.

References

- Li Z, Tang Y, Chen Y, Wang Y, Feng Y, Li Y and Wang F: Trends and Cross-country inequalities of melanoma and Non-melanoma skin cancer from 1990 to 2021 and predictive trends from 2022 to 2044: A global burden of disease study. *Life Conflux* 2: e284-e284, 2026.
- Schadendorf D, Van Akkooi AC, Berking C, Griewank KG, Gutzmer R, Hauschild A, Stang A, Roesch A and Ugurel S: Melanoma. *Lancet* 392: 971-984, 2018.
- Luke JJ, Flaherty KT, Ribas A and Long GV: Targeted agents and immunotherapies: Optimizing outcomes in melanoma. *Nat Rev Clin Oncol* 14: 463-482, 2017.
- Hayes JD, Dinkova-Kostova AT and Tew KD: Oxidative stress in cancer. *Cancer Cell* 38: 167-197, 2020.
- Gorrini C, Harris IS and Mak TW: Modulation of oxidative stress as an anticancer strategy. *Nat Rev Drug Discov* 12: 931-947, 2013.
- Vousden KH and Lane DP: p53 in health and disease. *Nat Rev Mol Cell Biol* 8: 275-283, 2007.
- Soengas MS and Lowe SW: Apoptosis and melanoma chemoresistance. *Oncogene* 22: 3138-3151, 2003.
- Rayman MP: The importance of selenium to human health. *Lancet* 356: 233-241, 2000.
- Hatfield DL, Tsuji PA, Carlson BA and Gladyshev VN: Selenium and selenocysteine: Roles in cancer, health, and development. *Trends Biochem Sci* 39: 112-120, 2014.
- Nilsson G, Sun X, Nyström C, Rundlöf AK, Fernandes AP, Björnstedt M and Dobra K: Selenite induces apoptosis in sarcomatoid malignant mesothelioma cells through oxidative stress. *Free Radic Biol Med* 41: 874-885, 2006.
- Wallenberg M, Misra S and Björnstedt M: Selenium cytotoxicity in cancer. *Basic Clin Pharmacol Toxicol* 114: 377-386, 2014.
- Gandin V, Khalkar P, Braude J and Fernandes AP: Organic selenium compounds as potential chemotherapeutic agents for improved cancer treatment. *Free Radic Biol Med* 127: 80-97, 2018.
- Doostan M, Rahmani Azar A, Azar A and Maleki H: Selenium nanoparticles and paclitaxel co-delivery by a PCL based nanofibrous scaffold to enhance melanoma therapy. *J Biomater Appl* 40: 165-180, 2025.
- Liao ZX, Ou DL, Hsu CL, Lu LN, Wen CH, Lu L, Chiu CL, Yang PC and Tseng SJ: Local M1 macrophage reprogramming with gluconic Acid-coated selenium nanoparticles. *Int J Nanomedicine* 20: 14439-14455, 2025.
- Alsubaie S, Merghani N, Abudawood M, Siddiqi NJ and Fatima S: Comparative mechanistic insights into Quercetin-loaded selenium nanoparticles and cisplatin in HCT116 cells. *ACS Omega* 10: 57123-57136, 2025.
- Anjum S, Hashim M, Imran M, Babur S, Adnan S, Hano C and Ibrahim WN: Selenium nanoparticles in cancer therapy: Unveiling cytotoxic mechanisms and therapeutic potential. *Cancer Rep (Hoboken)* 8: e70210, 2025.
- Sanmartín C, Plano D, Sharma AK and Palop JA: Selenium compounds, apoptosis and other types of cell death: An overview for cancer therapy. *Int J Mol Sci* 13: 9649-9672, 2012.
- Vinceti M, Filippini T and Wise LA: Environmental selenium and human health: An update. *Curr Environ Health Rep* 5: 464-485, 2018.
- Trachootham D, Alexandre J and Huang P: Targeting cancer cells by ROS-mediated mechanisms: A radical therapeutic approach? *Nat Rev Drug Discov* 8: 579-591, 2009.
- Perillo B, Di Donato M, Pezone A, Di Zazzo E, Giovannelli P, Galasso G and Migliaccio A: ROS in cancer therapy: The bright side of the moon. *Exp Mol Med* 52: 192-203, 2020.
- Vejselova Sezer C: Escin induces cell death in human skin melanoma cells through apoptotic mechanisms. *Toxicol Res (Camb)* 13: tfae124, 2024.
- Mosmann T: Rapid colorimetric assay for cellular growth and survival: Application to proliferation and cytotoxicity assays. *J Immunol Methods* 65: 55-63, 1983.
- Van Meerloo J, Kaspers GJ and Cloos J: Cell sensitivity assays: The MTT assay. *Methods Mol Biol* 731: 237-245, 2011.
- Valko M, Rhodes CJ, Moncol J, Izakovic MM and Mazur M: Free radicals, metals and antioxidants in oxidative stress-induced cancer. *Chem Biol Interact* 160: 1-40, 2006.
- Singh NP, McCoy MT, Tice RR and Schneider EL: A simple technique for quantitation of low levels of DNA damage in individual cells. *Exp Cell Res* 175: 184-191, 1988.
- Azqueta A and Collins AR: The essential comet assay: A comprehensive guide to measuring DNA damage and repair. *Arch Toxicol* 87: 949-968, 2013.
- Olive PL and Banáth JP: The comet assay: A method to measure DNA damage in individual cells. *Nat Protoc* 1: 23-29, 2006.
- Livak KJ and Schmittgen TD: Analysis of relative gene expression data using real-time quantitative PCR and the 2(-Delta Delta C(T)) method. *Methods* 25: 402-408, 2001.
- Vandesompele J, De Preter K, Pattyn F, Poppe B, Van Roy N, De Paepe A and Speleman F: Accurate normalization of real-time quantitative RT-PCR data by geometric averaging of multiple internal control genes. *Genome Biol* 3: RESEARCH0034, 2002.
- Roh JI, Lee J, Sung YH, Oh J, Hyeon DY, Kim Y, Lee S, Devkota S, Kim HJ, Park B and Nam T: Impaired AKT signaling and lung tumorigenesis by PIERCE1 ablation in KRAS-mutant non-small cell lung cancer. *Oncogene* 39: 5876-5887, 2020.
- Lian Y, Ding J, Zhang Z, Shi Y, Zhu Y, Li J, Peng P, Wang J, Fan Y, De W and Wang K: The long noncoding RNA Hoxa transcript at the distal tip promotes colorectal cancer growth partially via silencing of p21 expression. *Tumor Biology* 37: 7431-7440, 2016.
- Dirican E, Özcan H, Uzunçakmak SK and Takım U: Evaluation expression of the caspase-3 and caspase-9 apoptotic genes in schizophrenia patients. *Clin Psychopharmacol Neurosci* 21: 171-178, 2023.
- Dwivedi N, Mondal S, P K S, T S, Sachdeva K, Bathula C, K V, K S N, Damodar S, Dhar SK and Das M: Relative quantification of BCL2 mRNA for diagnostic usage needs stable uncontrolled genes as reference. *PLoS One* 15: e0236338, 2020.
- Singh P, Mitra P, Goyal T, Sharma S and Sharma P: Evaluation of DNA damage and expressions of DNA repair gene in occupationally lead exposed workers (Jodhpur, India). *Biol Trace Elem Res* 199: 1707-1714, 2021.
- Rebecca VW, Sondak VK and Smalley KS: A brief history of melanoma: From mummies to mutations. *Melanoma Res* 22: 114-122, 2012.
- Leonardi GC, Candido S, Falzone L, Spandidos DA and Libra M: Cutaneous melanoma and the immunotherapy revolution. *Int J Oncol* 57: 609-618, 2020.
- Chen T and Wong YS: Selenocysteine induces apoptosis of A375 human melanoma cells by activating ROS-mediated mitochondrial pathway and p53 phosphorylation. *Cell Mol Life Sci* 65: 2763-2775, 2008.
- Shaaban S, Althikrallah HA, Negm A, Elmaaty AA and Al-Karmalawy AA: Repurposed organoselenium tethered amidic acids as apoptosis inducers in melanoma cancer via P53, BAX, caspases-3, 6, 8, 9, BCL-2, MMP2, and MMP9 modulations. *RSC Adv* 14: 18576-18587, 2024.

39. Venza I, Venza M, Visalli M, Lentini G, Teti D and d'Alcontres FS: ROS as regulators of cellular processes in melanoma. *Oxid Med Cell Longev* 2021: 1208690, 2021.
40. Becker AL and Indra AK: Oxidative stress in melanoma: Beneficial antioxidant and pro-oxidant therapeutic strategies. *Cancers* 15: 3038, 2023.
41. Grek CL and Tew KD: Redox metabolism and malignancy. *Curr Opin Pharmacol* 10: 362-368, 2010.
42. Ghasemi P, Maddah A., Salehzadeh A, Ziamajidi N, Kalantary-Charvadeh A, Abbasalipourkabir R and Salehzadeh M: Study of oxidative stress and apoptotic genes in SW480 cell lines treated with selenium nanoparticles. *J Rep Pharm Sci* 13: e151064, 2025.
43. Weekley CM and Harris HH: Which form is that? The importance of selenium speciation and metabolism in the prevention and treatment of disease. *Chem Soc Rev* 42: 8870-8894, 2013.
44. Schomburg L: Selenium deficiency due to diet, pregnancy, severe illness, or covid-19-A preventable trigger for autoimmune disease. *Int J Mol Sci* 22: 8532, 2021.
45. Gorini F and Vassalle C: Selenium and selenoproteins at the intersection of type 2 diabetes and thyroid pathophysiology. *Antioxidants (Basel)* 11: 1188, 2022.
46. Krakowiak A and Pietrasik S: New insights into oxidative and reductive stress responses and their relation to the anticancer activity of selenium-containing compounds as hydrogen selenide donors. *Biology* 12: 875, 2023.
47. Barchielli G, Capperucci A and Tanini D: The role of selenium in pathologies: An updated review. *Antioxidants* 11: 251, 2022.
48. Xia Z, Gao N, Wang J, Yan L, Ma C, Wang K and Weng Y: Construction of prognostic model and tumor microenvironment landscape based on cuproptosis-related subtypes in melanoma. *Life Conflux* 2: e214-e214, 2025.
49. Garbarino O, Valenti GE, Monteleone L, Pietra G, Mingari M C, Benzi A, Bruzzone S, Ravera S, Leardi R, Farinini E, *et al*: PLX4032 resistance of patient-derived melanoma cells: Crucial role of oxidative metabolism. *Front Oncol* 13: 1210130, 2023.
50. Zhao X, Chen F and Li H: Metabolic reprogramming-a breakthrough point in overcoming resistance to BRAF mutant melanoma targeted therapy (Review). *Oncol Lett* 31: 184, 2026.
51. Cesi G, Walbrecht G, Zimmer A, Kreis S and Haan C: ROS production induced by BRAF inhibitor treatment rewires metabolic processes affecting cell growth of melanoma cells. *Mol Cancer* 16: 102, 2017.
52. Wang Y, He J, Lian S, Zeng Y, He S, Xu J, Luo L, Yang W and Jiang J: Targeting Metabolic-Redox nexus to regulate drug resistance: From mechanism to tumor therapy. *Antioxidants* 13: 828, 2024.
53. Vodenkova S, Azqueta A, Collins A, Dusinska M, Gaivao I, Møller P, Opattova A, Vodicka P, Godschalk RWL and Langie SAS: An optimized comet-based in vitro DNA repair assay to assess base and nucleotide excision repair activity. *Nat Protoc* 15: 3844-3878, 2020.
54. Ladeira C, Møller P, Giovannelli L, Gajski G, Haveric A, Bankoglu EE, Azqueta A, Gerić M, Stopper H, Cabêda J, *et al*: The comet assay as a tool in human biomonitoring studies of environmental and occupational exposure to chemicals-a systematic scoping review. *Toxics* 12: 270, 2024.
55. Soonnarong R, Tungsukruthai S, Nutho B, Rungrotmongkol T, Vinayanuwattikun C, Maluangnont T and Chanvorachote P: Titania nanosheets generates peroxynitrite for S-Nitrosylation and enhanced p53 function in lung cancer cells. *Pharmaceutics* 13: 1233, 2021.
56. Shahriari F, Barati M, Shahbazi S, Arani HZ, Dahmardnezhad M, Javidi MA and Alizade A: Hypericin and resveratrol anti-tumor impact through E-cadherin, N-cadherin, galectin-3, and BAX/BCL-ratio; possible cancer immunotherapy succor on Y79 retinoblastoma cells. *Precision Medical Sciences* 14: 104-112, 2025.
57. Abbas T and Dutta A: p21 in cancer: Intricate networks and multiple activities. *Nat Rev Cancer* 9: 400-414, 2009.
58. Brandl N, Seitz R, Sendtner N, Müller M and Gülow K: Living on the edge: ROS homeostasis in cancer cells and its potential as a therapeutic target. *Antioxidants (Basel)* 14: 1002, 2025.
59. Akter S, Madhuvilakku R, Kar AK, Nila IS, Liu P, Inuzuka H and Hong Y: Reactive oxygen species (ROS) in cancer: From mechanism to therapeutic implications. *Signal Transduct Target Ther* 11: 111, 2026.
60. Feng Q, Xu X and Zhang S: Nrf2 protein in melanoma progression, as a new means of treatment. *Pigment Cell Melanoma Res* 37: 247-258, 2024.
61. Tang D and Kang R: NFE2L2 and ferroptosis resistance in cancer therapy. *Cancer Drug Resist* 7: 41, 2024.
62. Li K, Fan C, Chen J, Xu X, Lu C, Shao H and Xi Y: Role of oxidative stress-induced ferroptosis in cancer therapy. *J Cell Mol Med* 28: e18399, 2024.
63. Benedusi M, Lee H, Lim Y and Valacchi G: Oxidative state in cutaneous melanoma progression: A question of balance. *Antioxidants* 13: 1058, 2024.
64. Lin W, Zhang J, Xu JF and Pi J: The advancing of selenium nanoparticles against infectious diseases. *Front Pharm* 12: 682284, 2021.
65. Shahabadi N, Zendeheشم S and Khademi F: Selenium nanoparticles: Synthesis, in-vitro cytotoxicity, antioxidant activity and interaction studies with ct-DNA and HSA, Hb and Cyt c serum proteins. *Biotechnol Rep* 30: e00615, 2021.
66. Shehata NS, Elwakil BH, Elshewemi SS, Ghareeb DA and Olama ZA: Selenium nanoparticles coated bacterial polysaccharide with potent antimicrobial and anti-lung cancer activities. *Sci Rep* 13: 21871, 2023.
67. Zhang J, Ye ZW, Townsend DM and Tew KD: Redox pathways in melanoma. *Adv Cancer Res* 162: 125-143, 2024.
68. Sahu M and Jain U: ROS-mediated therapeutic approach through oxidative stress and cell signalling modulation. *Crit Rev Oncol Hematol* 220: 105168, 2026.
69. Featherston T, Paumann-Page M and Hampton MB: Melanoma redox biology and the emergence of drug resistance. *Adv Cancer Res* 162: 145-171, 2024.
70. Rayman MP: Selenium intake, status, and health: A complex relationship. *Hormones* 19: 9-14, 2020.
71. Bai S, Zhang M, Tang S, Li M, Wu R, Wan S, Feng S, Chen L, Wei X and Feng S: Effects and impact of selenium on human health, a review. *Molecules* 30: 50, 2024.
72. Le Gal K, Ibrahim MX, Wiel C, Sayin VI, Akula MK, Karlsson Dalin MG, Akyürek LM, Lindahl P, Nilsson J and Bergo MO: Antioxidants can increase melanoma metastasis in mice. *Sci Transl Med* 7: 308re8, 2015.
73. Piskounova E, Agathocleous M, Murphy MM, Hu Z, Huddleston SE, Zhao Leitch AM, Johnson TM, DeBerardinis RJ and Morrison SJ: Oxidative stress inhibits distant metastasis by human melanoma cells. *Nature* 527: 186-191, 2015.
74. Paudel BB, Lewis JE, Hardeman KN, Hayford CE, Robbins CJ, Stauffer PE, Codreanu SG, Sherrod SD, McLean JA, Kemp ML and Quaranta V: An integrative gene expression and mathematical flux balance analysis identifies targetable redox vulnerabilities in melanoma cells. *Cancer Res* 80: 4565-4577, 2020.
75. Ranbhise JS, Singh MK, Ju S, Han S, Yun HR, Kim SS and Kang I: The redox paradox: Cancer's double-edged sword for malignancy and therapy. *Antioxidants (Basel)* 14: 1187, 2025.
76. Jia X, Wang Y, Qiao Y, Jiang X and Li J: Nanomaterial-based regulation of redox metabolism for enhancing cancer therapy. *Chem Soc Rev* 53: 11590-11656, 2024.
77. Hosnedlova B, Kepinska M, Skalickova S, Fernandez C, Ruttkay-Nedecky B, Peng Q, Baron M, Melcova M, Opatrilova R, Zidkova J, *et al*: Nano-selenium and its nanomedicine applications: A critical review. *Int J Nanomedicine* 13: 2107-2128, 2018.
78. Fernandes AP and Gandin V: Selenium compounds as therapeutic agents in cancer. *Biochim Biophys Acta* 1850: 1642-1660, 2015.
79. Nie S, He X, Sun Z, Zhang Y, Liu T, Chen T and Zhao J: Selenium speciation-dependent cancer radiosensitization by induction of G2/M cell cycle arrest and apoptosis. *Front Bioeng Biotechnol* 11: 1168827, 2023.
80. Kuršvietienė L, Mongirdienė A, Bernatoniene J, Šulinskienė J and Stanevičienė I: Selenium anticancer properties and impact on cellular redox status. *Antioxidants (Basel)* 9: 80, 2020.
81. Bansal MP: Redox regulation and therapeutic approaches in cancer. *Springer*, Dec 13, 2023. <https://doi.org/10.1007/978-981-99-7342-2>.
82. Liang X, Weng J, You Z, Wang Y, Wen J, Xia Z, Huang S, Luo P and Cheng Q: Oxidative stress in cancer: From tumor and micro-environment remodeling to therapeutic frontiers. *Mol Cancer* 24: 219, 2025.

